Volume 24
Number 2
14 January 2026
Pages 243-518

Organic & Biomolecular Chemistry

rsc.li/obc

ISSN 1477-0520

ROYAL SOCIETY OF CHEMISTRY

COMMUNICATION
Michaela E. Everly and Patrick J. Hrdlicka
Efficient and specific DNA-targeting using single-stranded LNA/MOE mixmers and chimeric Invader:XenoRNA probes

Organic & Biomolecular Chemistry

ROYAL SOCIETY OF CHEMISTRY

COMMUNICATION

View Article Online
View Journal | View Issue

Cite this: *Org. Biomol. Chem.*, 2026, **24**, 319

Received 30th September 2025,
Accepted 15th October 2025

DOI: 10.1039/d5ob01570g

rsc.li/obc

Efficient and specific DNA-targeting using single-stranded LNA/MOE mixmers and chimeric Invader:XenoRNA probes

Michaela E. Everly and Patrick J. Hrdlicka *

DNA-targeting properties of heteroduplexes between intercalator-functionalized oligonucleotides and various Xeno RNAs (*i.e.*, LNA/MOE mixmers, or fully modified MOE, O2′-Me, or 2′-F strands) are disclosed. Chimeric Invader:LNA/MOE probes and some single-stranded LNA/MOE mixmers enable efficient invasion of double-stranded DNA targets with exceptional binding specificity.

Nucleic acid-based therapeutics are transforming modern medicine. However, while over twenty RNA-targeting modalities have received FDA approval, no DNA-targeting oligonucleotides (ONs) have reached the clinic, as chromosomal DNA is a more challenging target. To realize sequence-specific recognition of double-stranded DNA (dsDNA), probes must invade Watson-Crick base pairs (bps) or bind *via* the duplex grooves, with polyamides,[1] and triplex forming oligonucleotides[2] and peptide nucleic acids (PNAs)[3] being representative examples of the latter. However, groove binders are limited in targeting scope (*e.g.*, triplex formation is generally restricted to polypurine regions). Strand-invading probes such as single-stranded modified PNAs[4–8] and locked nucleic acids (LNAs),[9,10] or various double-stranded probes (dsProbes),[11–15] can target and unzip Watson-Crick bps of dsDNA targets to form more stable bps between individual probe strands and complementary DNA (cDNA). While capable of targeting mixed-sequence dsDNA regions, single-stranded (ss) strand-invading probes modified with affinity-enhancing modifications often form secondary structures that compromise binding efficiency, whereas dsProbes must be engineered to denature easily whilst maintaining high cDNA affinity.

In pursuit of improved strategies for mixed-sequence dsDNA-recognition, we have explored *Invader probes*,[16,17] *i.e.*, dsProbes with +1 interstrand zipper arrangements† of intercalator-functionalized nucleotides like 2′-*O*-(pyren-1-yl)methyl-RNA (Fig. 1). This arrangement forces pyrene moieties between the π-stacks of neighboring bps, resulting in violation of the nearest neighbor exclusion principle[18,19] (NNEP) and duplex destabilization.‡ Conversely, the individual probe strands display high affinity towards cDNA as duplex formation results in pyrene intercalation and strongly stabilizing stacking interactions with flanking bps (NNEP is not violated, Fig. 1). The difference in stability drives dsDNA-invasion, and has been used to enable detection of various biological targets.[16,17,20,21] As an extension of our original strategy, we recently introduced *chimeric Invader probes*, *i.e.*, heteroduplexes between densely modified Invader strands and complementary strands of miniPEG-γPNA (^{MP}γPNA), serine-γPNA (^{Ser}γPNA), or LNA.[22–24] This strategy was inspired by prior studies on DNA-targeting heteroduplex probes between intercalator-modified ONs and complementary RNA, PNA, or LNA strands,[25–27] and relies on the observation that intercalators are often poorly accommodated in PNA/DNA and *A*-type (RNA-like) duplexes,[28,29] but well-tolerated in *B*-type (DNA-like) duplexes. The chimeric Invader probes were found to be activated for dsDNA-invasion, with more efficient and specific recognition than the corresponding ssProbes.[22–24]

Here, we describe the dsDNA-recognition properties of new chimeric probe designs consisting of densely modified Invader

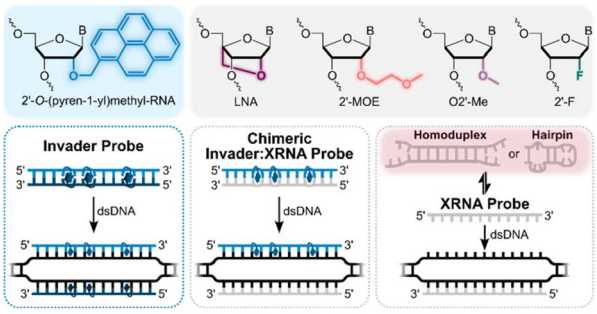

Fig. 1 Structures of monomers used herein and illustrations of dsDNA-invasion using Invader, chimeric Invader:XRNA, or ssXRNA probes. XRNAs (grey) are LNA/MOE mixmers or fully modified MOE, O2′-Me, or 2′-F strands.

Department of Chemistry, University of Idaho, Moscow, Idaho 83844-2343, USA. E-mail: hrdlicka@uidaho.edu

strands and complementary Xeno RNAs (XRNAs), *i.e.*, fully modified 2′-*O*-methoxyethyl (MOE), 2′-*O*-methyl (O2′-Me), 2′-Fluoro (2′-F) or LNA/MOE mixmers.

Fourteen 13-mer probes – seven double-stranded chimeric probes and seven ssXRNAs – were designed to target a model dsDNA target and evaluated against the corresponding conventional Invader and chimeric Invader:LNA probes (Table 1).[24] Different LNA/MOE mixmer designs were studied to determine if the relative placement of LNA and MOE monomers *vis-à-vis* the pyrene-functionalized monomers impacts dsDNA-invasion. Thus, LNA or MOE monomers were incorporated as blocks ("blks") of 2–4 residues, positioned across from the Invader monomers, or in a systematically alternating ("alt") fashion with either LNA or MOE monomers across from the Invader monomers (Table 1).

As expected, individual XRNA and Invader strands form stable duplexes with cDNA (thermal denaturation temperatures (T_ms) = 46.0–77.0 °C), with the order of stability decreasing as follows: alt LNA/MOE ≥ LNA > blk LNA/MOE > Invader > 2′-F ~ MOE > O2′-Me (Table 1). Conversely, the stability of the conventional Invader probe **INVu:INVd** is lower than the corresponding duplexes between individual Invader strands and cDNA (T_m = 51.0 °C *vs.* 61.0–63.0 °C). The term *thermal advantage* (TA), calculated as TA = T_m (upper strand *vs.* cDNA) + T_m (lower strand *vs.* cDNA) − T_m (probe duplex) − T_m (dsDNA), is a measure of the available driving force for recognition of complementary dsDNA regions, with more positive TA values indicating a stronger driving force.[16] Prior studies have demonstrated that conventional and chimeric Invader probes resulting in efficient dsDNA-recognition display substantially positive TA values. **INVu:INVd** displays a favorable TA value of 35.5 °C. The chimeric Invader:LNA probe **LNA1:INVd** displays an even more favorable TA value of 65.0 °C, as the probe is far more labile (T_m = 31.5 °C). The chimeric Invader:LNA/MOE probes display irregular denaturation profiles indicative of perturbed duplex geometries, rendering accurate T_m and TA determination challenging. Thus, **blkMOE1:INVd** and **altMOE4:INVd** do not have clear transitions, while **blkMOE2:INVd** and **altMOE3:INVd** have high-melting irregular transitions (T_ms = 73.0–74.5 °C), resulting in moderate TA values of 22.0–23.5 °C. Chimeric probes entailing the fully modified MOE, O2′-Me, or 2′-F are more stable than the corresponding Invader probes (T_ms = 53.0–59.0 °C), and also result in moderate TA values of 18.5–25.0 °C. Analysis of pyrene absorbance trends, suggests

Table 1 Sequences of probes; T_ms of probe duplexes and duplexes between individual probe strands and cDNA, and TA values[a]

Name	dsProbe	T_m [ΔT_m] (°C) ssXRNA Strand	Probe duplex	5′-Strand *vs.* cDNA	3′-Strand *vs.* cDNA	dsProbe TA (°C)
blkMOE1 INVd	5′-GGTATATATAGGC-3′ 3′-CCAUAUAUATAUCCG-5′	>80.0 [>+42.5]	—[b]	66.5[c] [+29.0]	63.0 [+25.5]	n.d.
blkMOE2 INVd	5′-GGTATATATAGGC-3′ 3′-CCAUAUAUATAUCCG-5′	53.0 [+15.5]	73.0 [+35.5]	69.5 [+32.0]	63.0 [+25.5]	22.0
altMOE3 INVd	5′-GGTATATATAGGC-3′ 3′-CCAUAUAUATAUCCG-5′	73.5 [+36.0]	74.5[b] [+37.0]	72.5[c] [+35.0]	63.0 [+25.5]	23.5
altMOE4 INVd	5′-GGTATATATAGGC-3′ 3′-CCAUAUAUATAUCCG-5′	>80.0 [>+42.5]	—[b]	~77.0[c] [+39.5]	63.0 [+25.5]	n.d.
fullMOE INVd	5′-GGTATATATAGGC-3′ 3′-CCAUAUAUATAUCCG-5′	34.5 [−3.0]	53.0 [+15.5]	52.5 [+15.0]	63.0 [+25.5]	25.0
fullOMe INVd	5′-GGUAUAUAUAGGC-3′ 3′-CCAUAUAUATAUCCG-5′	24.0 [−13.5]	53.0 [+15.5]	46.0 [+8.5]	63.0 [+25.5]	18.5
fullF INVd	5′-GGUAUAUAUAGGC-3′ 3′-CCAUAUAUATAUCCG-5′	28.0 [−9.5]	59.0 [+21.5]	54.0 [+16.5]	63.0 [+25.5]	20.5
INVu INVd[d]	5′-GGUAUATAUAGGC-3′ 3′-CCAUAUAUATAUCCG-5′	n.d.	51.0 [+13.5]	61.0 [+23.5]	63.0 [+25.5]	35.5
LNA1 INVd[d]	5′-GGTATATATAGGC-3′ 3′-CCAUAUAUATAUCCG-5′	>80.0 [>+42.5]	31.5 [−6.0]	71.0 [+33.5]	63.0 [+25.5]	65.0

[a] 2′-*O*-(Pyren-1-yl)methyluridine, LNA, MOE, O2′-Me, 2′-F, and unmodified DNA monomers represented as blue, dark purple, peach, light purple, green, and grey circles, respectively. LNA and MOE "C" = 5-methyl-cytosin-1-yl monomer. ΔT_m = change in T_m relative to unmodified DNA duplex 5′-GGTATATATAGGC : 3′-CCATATATATCCG (T_m = 37.5 °C). T_ms were recorded in medium salt phosphate buffer ([Na^+] = 110 mM, [Cl^-] = 100 mM, pH 7.0 (NaH_2PO_4/Na_2HPO_4), [EDTA] = 0.2 mM) using 1.0 μM of each strand. "n.d." = not determined. [b] Irregular profiles and/or broad transitions (Fig. S1 and S2). [c] T_ms determined from differential thermal denaturation curves (Fig. S2). [d] Previously reported in ref. 21 and 24.

that XRNA modifications – contrary to expectations – do not deter pyrene intercalation (Fig. S4, Table S3, and associated discussion), resulting in the high stability of chimeric probes.

Thermal denaturation profiles were also recorded for the ssXRNAs in absence of cDNA to assess if stable secondary structures are formed in the partially self-complementary, AT-rich sequence context, as this could interfere with duplex formation. Indeed, clear transitions were observed in all cases (Table 1, Fig. S1). Fully MOE, O2′-Me, and 2′-F modified XRNAs form weakly stable secondary structures (T_ms = 24.0–34.5 °C), whereas three of four LNA/MOE strands form very stable secondary structures (T_ms > 73.5 °C); **blkMOE2** forms a moderately stable secondary structure (T_m = 53.0 °C; Table 1). Denaturation experiments, in which the XRNA concentration was increased 10-fold, were conducted to gain insight into the type of secondary structure formed. All XRNAs, except for **blkMOE1**, displayed increased T_ms at higher concentrations, suggesting that homoduplexes are formed (Fig. 2, Fig. S3, Table S1).

The greater stability of the secondary structures observed for **altMOE3** and **altMOE4** *vis-à-vis* **blkMOE2** may reflect their greater number of affinity-enhancing LNA monomers in the self-complementary region. **blkMOE1** did not result in an increased T_m with higher strand concentrations, pointing to formation of a stable intramolecular hairpin (Fig. 2, Fig. S3, Table S1). The modification pattern of **blkMOE1** appears to favor intramolecular interactions. We speculate that this is due to the formation of stable LNA:LNA bps in the center of the hairpin structure (Fig. 2). Hairpin formation by the other LNA/MOE mixmers would likely require formation of two MOE:LNA or MOE:MOE bps (Fig. 2), which might not be sufficiently stable to promote hairpin formation.

The dsDNA-targeting properties of the chimeric Invader:XRNA probes and ssXRNAs were evaluated using an established electrophoretic mobility shift assay (EMSA) that relies on a chemiluminescent readout.[30] A 5-fold molar excess of probe was incubated with a digoxigenin (DIG)-labeled DNA hairpin (**DH1**) comprised of a 13-mer double-stranded target region (complementary to the probes) linked at one end by a T_{10} loop. The unimolecular nature of **DH1** renders it a high-melting target (T_m = 58.5 °C; Table S5). Successful invasion of **DH1** by ssProbes or dsProbes is expected to form binary or ternary invasion complexes, respectively, with reduced electrophoretic mobility on non-denaturing polyacrylamide gels relative to unbound **DH1** (Fig. 3a).

Conventional Invader probe **INVu:INVd** and chimeric Invader:LNA probe **LNA1:INVd** resulted in substantial invasion of **DH1** (~95%; Fig. 3b). Conversely, individual Invader strands only result in trace invasion of **DH1**,[24] while **LNA1** resulted in more moderate invasion (~55%; Fig. 3b). Three of four chimeric Invader:LNA/MOE probes resulted in substantial invasion (>85%; Fig. 3c), while invasion was more moderate with **blkMOE2:INVd** (~40%; Fig. 3c), in line with TA (Table 1) and ΔG_{rec} values (Table S2). Unexpectedly, three of four single-stranded LNA/MOE mixmers resulted in efficient invasion of **DH1** (>85%; Fig. 3c), while invasion with **altMOE4** was more moderate (~50%; Fig. 3c), likely due to its formation of a stable homoduplex (T_m > 80 °C; Table 1). The chimeric probes entailing the fully MOE, O2′-Me and 2′-F strands resulted in moderate **DH1** invasion (30–65%; Fig. 3b) in agreement with their less favorable TA (Table 1) and ΔG_{rec} values (Table S2), whereas the individual probe strands resulted in little to no recognition.

Next, the dsDNA-binding specificities of the chimeric Invader:LNA/MOE probes and the single-stranded LNA/MOE mixmers were evaluated. Thus, a 25-fold molar excess of each probe was incubated with DNA hairpins **DH2–DH7**, which only differ at position 6 or 9 (a or b, respectively, Fig. 4) of the

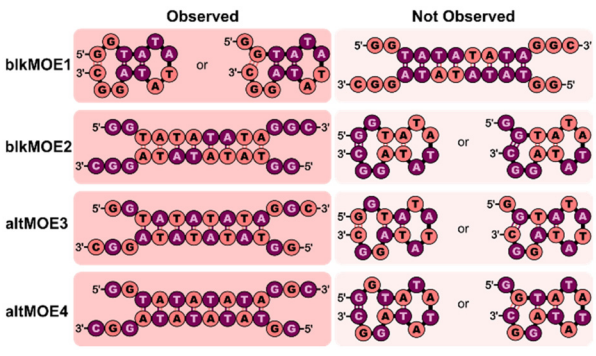

Fig. 2 Predicted secondary structures formed by single-stranded LNA/MOE mixmers. Color scheme as in Table 1.

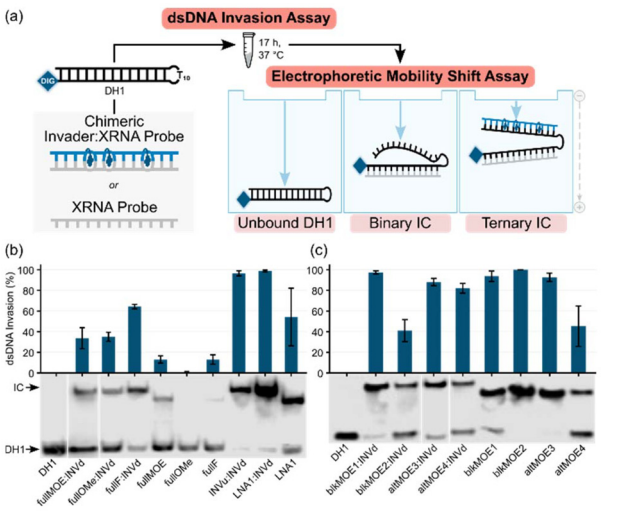

Fig. 3 (a) Assays used to evaluate dsDNA-invasion by chimeric Invader:XRNA or ssXRNA probes. (b and c) Representative electrophoretograms for invasion experiments with DIG-labeled **DH1** and various probes (left lanes contain DIG-**DH1** only). Histograms depict mean percent of **DH1** invasion; error bars denote standard deviation from at least three experiments. IC = invasion complex. DIG-**DH1** (50 nM, 5′-GGTATATATAGGC-T_{10}-GCCTATATATACC-3′) was incubated with probe in HEPES buffer (50 mM HEPES, 100 mM NaCl, 5 mM $MgCl_2$, pH 7.2, 10% sucrose, 1.44 mM spermine tetrahydrochloride) at 37 °C for ~17 h. Mixtures were resolved on 20% nd-PAGE gels. Electrophoretograms are composites of two separate gels.

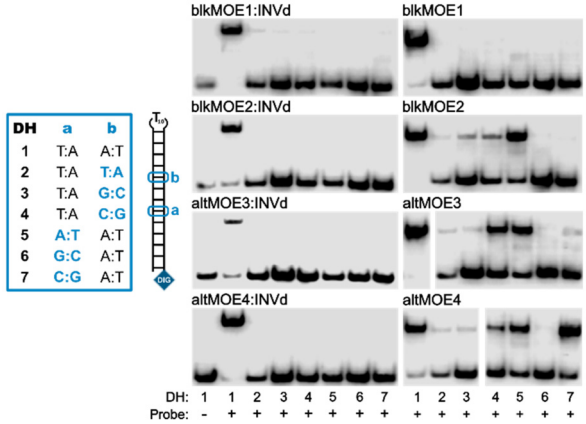

Fig. 4 Representative electrophoretograms from specificity experiments. **DH1–DH7** were incubated with a 25-fold molar probe excess. For sequences and T_ms of **DH1–DH7**, see Table S5. Experimental conditions as in Fig. 3. The electrophoretograms for **altMOE3** and **altMOE4** are from one gel, with an irrelevant lane excised.

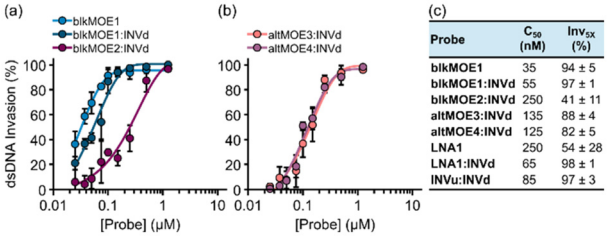

Fig. 5 (a and b) Dose–response curves for invasion of **DH1** by **blkMOE1** and chimeric Invader:LNA/MOE probes. For representative electrophoretograms, see Fig. S6; experimental conditions as in Fig. 3. (c) C_{50} values and percent **DH1** invasion when using 5-fold probe excess (Inv_{5X}). For Inv_{5X} data for **blkMOE2**, **altMOE3**, **altMOE4**, and the probes entailing fully modified XRNAs, see Table S4; "±" = standard deviation from at least three trials. Data for **LNA1**:**INVd** and **INVu**:**INVd** are from ref. 24.

double-stranded region relative to the probes. Akin to our prior observations with conventional Invader, chimeric Invader:LNA, and chimeric Invader:γPNA probes,[22–24] every chimeric Invader:LNA/MOE probes displayed outstanding binding specificity as evidenced by the (near-)complete absence of **DH2–DH7** invasion (Fig. 4), at conditions resulting in (near-)complete invasion of **DH1** (Fig. 4). In contrast – and similar to our prior observations with single-stranded LNA,[24] γPNA, and ^{Ser}γPNA probes[22,23] – three of the four LNA/MOE mixmers result in substantial non-specific recognition of **DH2–DH7** (Fig. 4). Interestingly, LNA/MOE mixmer **blkMOE1** displayed near-perfect discrimination of **DH2–DH7** (Fig. 4). Presumably, the excellent binding specificity of the chimeric Invader:LNA/MOE probes is due to stringency clamping effects that are often observed with structured metastable probes.[31] Binding to incorrect dsDNA targets would require (i) denaturation of both the dsProbe and dsDNA target region, and (ii) formation of two less stable, mismatched duplexes in the invasion complexes.[32] A similar effect might explain the excellent binding specificity of **blkMOE1**. Thus, the intramolecular hairpin formed by **blkMOE1** is likely more stable than the complexes formed with mismatched DNA hairpins, but less stable than the complex formed with the fully matched **DH1**, whereas the secondary structures formed by the other single-stranded LNA/MOE mixmers are less stable than the complexes formed with the fully matched and mismatched DNA hairpins, resulting in poor binding specificity.

Informed by the results from the initial screen and specificity experiments, the four chimeric Invader:LNA/MOE probes and the single-stranded LNA/MOE mixmer **blkMOE1** were selected for dose–response experiments to determine C_{50} values, *i.e.*, the probe concentration resulting in 50% recognition of **DH1** (Fig. 5). The four chimeric Invader:LNA/MOE probes displayed C_{50} values below 250 nM, with **blkMOE1**:**INVd** displaying a comparable C_{50} value to the corresponding conventional Invader and chimeric Invader:LNA probes (C_{50} = 55–85 nM). Remarkably, **blkMOE1** resulted in near-stoichiometric recognition of **DH1** (C_{50} = 35 nM; Fig. 5).

In conclusion, these results suggest that chimeric Invader:LNA/MOE probes have considerable promise for efficient and highly specific recognition of dsDNA targets. Perhaps even more exciting – given their structural simplicity and commercial availability – is the prospect of using single-stranded LNA/MOE mixmers for mixed-sequence dsDNA-invasion. Further studies are needed to determine the robustness of this strategy, but the high binding efficiency and specificity observed with **blkMOE1** is promising. Results from such studies will be reported in due course.

Conflicts of interest

PJH is an inventor on patents pertaining to Invader probes, which have been issued to the University Idaho.

Data availability

The data supporting this article have been included as part of the supplementary information (SI). Supplementary information is available. See DOI: https://doi.org/10.1039/d5ob01570g.

Acknowledgements

This publication was made possible by an Institutional Development Award (IDeA) from the National Institute of General Medical Sciences of the National Institutes of Health under Grant #P20GM103408.

References

† For interstrand zipper nomenclature definition, see SI.
‡ For a more detailed explanation of the NNEP, see SI.

1 Y. Kawamoto, T. Bando and H. Sugiyama, *Bioorg. Med. Chem.*, 2018, **26**, 1393–1411.
2 Y. Mikame and A. Yamayoshi, *Pharmaceutics*, 2023, **15**, 2515.
3 N. Brodyagin, M. Katkevics, V. Kotikam, C. A. Ryan and E. Rozners, *Beilstein J. Org. Chem.*, 2021, **17**, 1641–1688.
4 A. Dragulescu-Andrasi, S. Rapireddy, B. M. Frezza, C. Gayathri, R. R. Gil and D. H. Ly, *J. Am. Chem. Soc.*, 2006, **128**, 10258–10267.
5 R. Bahal, B. Sahu, S. Rapireddy, C.-M. Lee and D. H. Ly, *ChemBioChem*, 2012, **13**, 56–60.
6 P. R. Bohländer, T. Vilaivan and H.-A. Wagenknecht, *Org. Biomol. Chem.*, 2015, **13**, 9223–9230.
7 S. A. Thadke, V. M. Hridya, J. D. R. Perera, R. R. Gil, A. Mukherjee and D. H. Ly, *Commun. Chem.*, 2018, **1**, 79.
8 H. Zheng, I. Botos, V. Clausse, H. Nikolayevskiy, E. E. Rastede, M. F. Fouz, S. J. Mazur and D. H. Appella, *Nucleic Acids Res.*, 2021, **49**, 713–725.
9 K. M. L. Hertoghs, J. H. Ellis and I. R. Catchpole, *Nucleic Acids Res.*, 2003, **31**, 5817–5830.
10 E. M. Zaghloul, A. S. Madsen, P. M. D. Moreno, I. I. Oprea, S. El-Andaloussi, B. Bestas, P. Gupta, E. B. Pedersen, K. E. Lundin, J. Wengel and C. I. E. Smith, *Nucleic Acids Res.*, 2011, **39**, 1142–1154.
11 Y. Aiba, M. Shibata and O. Shoji, *Appl. Sci.*, 2022, **12**, 3677.
12 J. Lohse, O. Dahl and P. E. Nielsen, *Proc. Natl. Acad. Sci. U. S. A.*, 1999, **96**, 11804–11808.
13 Y. Aiba, Y. Honda and M. Komiyama, *Chem. – Eur. J.*, 2015, **21**, 4021–4026.
14 M. López-Tena, L. Farrera-Soler, S. Barluenga and N. Winssinger, *JACS Au*, 2023, **3**, 449–458.
15 V. V. Filichev, B. Vester, L. H. Hansen and E. B. Pedersen, *Nucleic Acids Res.*, 2005, **33**, 7129–7137.
16 D. C. Guenther, G. H. Anderson, S. Karmakar, B. A. Anderson, B. A. Didion, W. Guo, J. P. Verstegen and P. J. Hrdlicka, *Chem. Sci.*, 2015, **6**, 5006–5015.
17 C. P. Shepard, R. G. Emehiser, S. Karmakar and P. J. Hrdlicka, *Molecules*, 2023, **28**, 127.
18 H. Ihmels and D. Otto, *Top. Curr. Chem.*, 2005, **258**, 161204.
19 O. Persil and N. V. Hud, *Trends Biotechnol.*, 2007, **25**, 433–436.
20 B. Denn, S. Karmakar, D. C. Guenther and P. J. Hrdlicka, *Chem. Commun.*, 2013, **49**, 9851–9853.
21 R. Emehiser, E. Hall, D. C. Guenther, S. Karmakar and P. J. Hrdlicka, *Org. Biomol. Chem.*, 2020, **18**, 56–65.
22 R. G. Emehiser and P. J. Hrdlicka, *Org. Biomol. Chem.*, 2020, **18**, 1359–1368.
23 R. G. Emehiser, K. Dhuri, C. Shepard, S. Karmakar, R. Bahal and P. J. Hrdlicka, *Org. Biomol. Chem.*, 2022, **20**, 8714–8724.
24 M. E. Everly, R. G. Emehiser and P. J. Hrdlicka, *Org. Biomol. Chem.*, 2025, **23**, 619–628.
25 T. Bryld, T. Højland and J. Wengel, *Chem. Commun.*, 2004, 1064–1065.
26 V. V. Filichev, U. B. Christensen, E. B. Pedersen, B. R. Babu and J. Wengel, *ChemBioChem*, 2004, **5**, 1673–1679.
27 H. Asanuma, R. Niwa, M. Akahane, K. Murayama, H. Kashida and Y. Kamiya, *Bioorg. Med. Chem.*, 2016, **24**, 4129–4137.
28 P. Wittung, S. K. Kim, O. Buchardt, P. Nielsen and B. Norden, *Nucleic Acids Res.*, 1994, **22**, 5371–5377.
29 V. Marin, H. F. Hansen, T. Koch and B. A. Armitage, *J. Biomol. Struct. Dyn.*, 2004, **21**, 841–850.
30 M. E. Everly, P. J. Wieber, I. Al Janabi and P. J. Hrdlicka, An electrophoretic mobility shift assay with chemiluminescent readout to evaluate DNA-targeting oligonucleotide-based probes, *protocols.io*, 2025. DOI: 10.17504/protocols.io.4r3l218rxg1y/v1.
31 V. V. Demidov and M. D. Frank-Kamenetskii, *Trends Biochem. Sci.*, 2004, **29**, 62–71.
32 S. X. Chen, D. Y. Zhang and G. Seelig, *Nat. Chem.*, 2013, **5**, 782–789.